Nanoscale

Accepted Manuscript

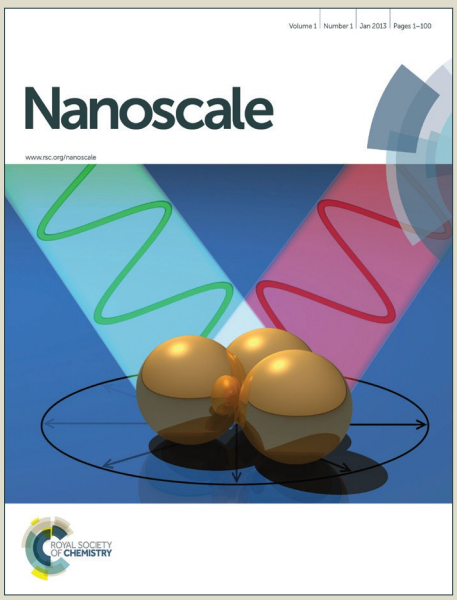

ROYAL SOCIETY OF CHEMISTRY

www.rsc.org/nanoscale

Journal Name

COMMUNICATION

Functionalized graphene nanomaterials: new insight into direct exfoliation of graphite with supramolecular polymers

Received 00th January 20xx,
Accepted 00th January 20xx

DOI: 10.1039/x0xx00000x

www.rsc.org/

Chih-Chia Cheng,*[a] Feng-Chih Chang,[b] Jui-Hsu Wang,[b] Jem-Kun Chen,[c] Ying-Chieh Yen,[d] Duu-Jong Lee[e,f]

A novel urea-cytosine-mimetic supramolecular polymer (UrCy-PPG) can self-assemble into a long-range ordered lamellar microstructure on the surface of graphene, due to the strong specific interactions between UrCy-PPG and graphene. In addition, the graphene composite produced exhibits a high conductivity (~1093 S/m) with a dramatic thermo-responsive ON/OFF resistance-switching behavior (10 consecutive cycles).

Graphene is a two-dimensional allotropic form of carbon comprised of a single atom-thick hexagonal lattice of carbon atoms linked by sp^2 covalent bonds. Graphene has attracted considerable interest due to its extraordinary features, such as its mechanical, thermal and electronic properties,[1-4] and has significant potential for various applications including electronic devices, energy storage and biomedicine.[5] Therefore, the ability to produce high quality, defect-free graphene has been a major area of research in the last several years. However, due to the lack of methods for efficient, cost-effective, large-scale production, the practical use of graphene is limited. Thus, many ingenious techniques have been developed to produce graphene using synthesis approaches, such as exfoliation of graphite in the liquid phase,[6-7] graphene oxide reduction[8] and chemical vapor deposition (CVD)[9,10] as representative methods. Exfoliation of graphite in the liquid phase has attracted a great deal of attention in recent years because of its advantages of easier scale-up for low-cost production of highly-conductive graphene in comparison with standard CVD-grown processes. Although the exfoliation of graphite has provided a convenient method of making graphene from graphite, it still remains a great challenge to obtain high concentrations of uniform graphene. [11]

Non-covalent functionalization is preferable for exfoliation of graphite in certain organic solvents, as it enables the attachment of specific molecules through π–stacking and hydrophobic interactions while still preserving the intrinsic physical properties of graphene.[12-15] Non-covalent functionalization has recently been incorporated into oligomers to form supramolecular polymers, which exhibit tailored properties and reversibility of the bonds between the monomeric units.[16-17] Using these supramolecular polymers, manipulation and well-controlled dispersion of carbon nanotubes can be easily achieved.[18-20] Despite these successful developments, the direct exfoliation of graphite to graphene by employing non-covalent interactions within supramolecular polymers has not yet been reported. Herein, we describe the preparation of stable, high-concentration graphene dispersions by direct exfoliation of graphite promoted by the efficient interactions between urea-cytosine end-capped polypropylene glycol (UrCy-PPG) and graphene in organic media.

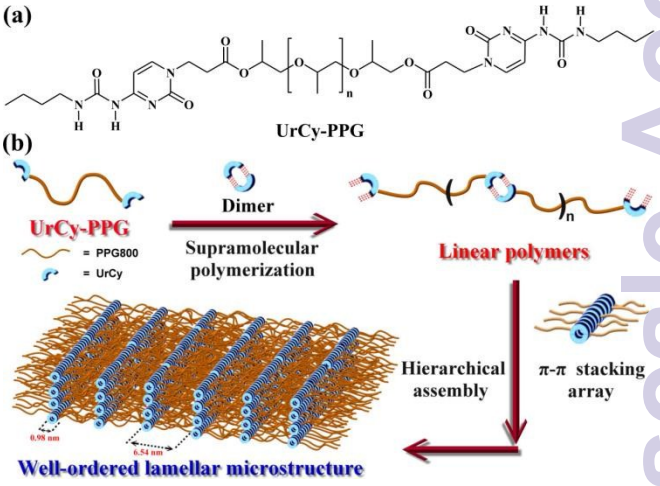

Scheme 1. (a) Chemical structures of the UrCy-PPG macromer. **(b)** Illustration of the self-assembly process of UrCy-PPG self-assembled complexes in the bulk state.

We recently developed a new UrCy-PPG macromer for the synthesis of a high-quality supramolecular polymer at kilogram scale.[21] This newly-developed material contains urea-cytosine (UrCy) moieties with a high association constant ($K_a > 10^6$ M^{-1}) and exhibits excellent self-assembly properties in solution and solid state. It has been suggested that UrCy-PPG can be further concentrated

[a] Graduate Institute of Applied Science and Technology, National Taiwan University of Science and Technology, Taipei 10607, Taiwan. E-mail: ccheng@mail.ntust.edu.tw
[b] Institute of Applied Chemistry, National Chiao Tung University, Hsin Chu 30050, Taiwan.
[c] Department of Materials Science and Engineering, National Taiwan University of Science and Technology, Taipei 10607, Taiwan.
[d] Department of Chemical and Biomolecular Engineering, The Ohio State University, Columbus, Ohio 43210, USA
[e] Department of Chemical Engineering, National Taiwan University, Taipei 10617, Taiwan.
[f] Department of Chemical Engineering, National Taiwan University of Science and Technology, Taipei 10607, Taiwan.

Electronic Supplementary Information (ESI) available: Experimental part including analytical methods synthesis procedures, spectral characterizations and related data. See DOI: 10.1039/x0xx00000x

assembled into a long-range ordered lamellar microstructure with a layer spacing of ca. 7 nm (Scheme 1). In this study, we demonstrate that this macromer can also be used to directly exfoliate graphite into graphene in tetrahydrofuran (THF) without extra chemical or centrifugal treatments. Moreover, this new process produces high-quality graphene flakes in which the layer number can not only be rigorously controlled, but the resulting graphene also exhibits superior electrical conductivity and resistive switching behavior; hence, this represents an entirely new, high-efficiency, cost-effective approach for the exfoliation of graphite. This study may help to address some fundamental questions regarding the production of graphene: Is the exfoliation of graphite induced by specific interactions with UrCy-PPG? Can we use this system to obtain the desired thickness of graphene? Does this study provide new concepts for directly exfoliating graphene from graphite?

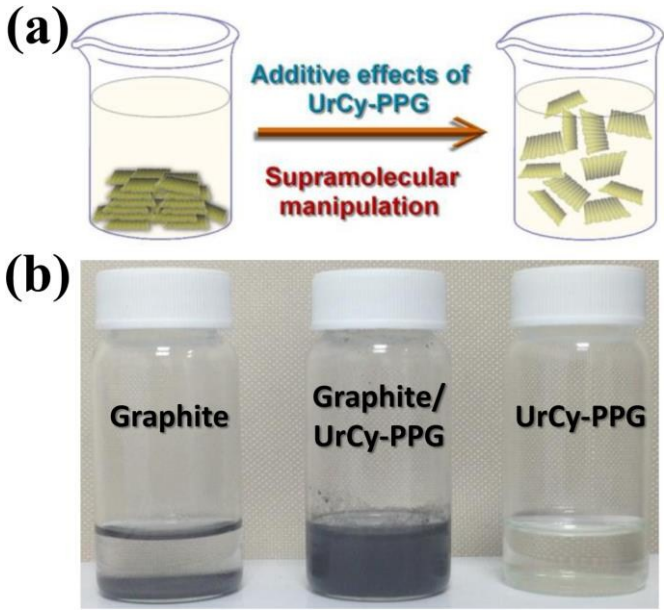

Scheme 2. (a) Schematic illustration of the direct exfoliation of graphite in organic solvent with UrCy-PPG. **(b)** Photographs of dispersed graphite in THF solution, after ultrasonic treatment at 30 ℃ for 3 h.

The preparation route for graphite/UrCy-PPG composites is shown in Scheme 2a, and is based on a blending method by exfoliating graphite via its interaction with UrCy-PPG in THF solvent. Because of the large amount of graphite powder addition (30-70 wt%) needed to break the van der Waals' forces of attraction between adjacent graphite layers, increasing the sonication time seems to be an important procedure to enhance the interaction between UrCy-PPG and graphite materials. After ultrasonic treatment at 25 ℃ for 3 h, the blends are dispersed into the solvent and form a black suspension (Scheme 2b). Then, subsequent solvent evaporation results in hybrid composites *without further purification*. It was interesting to understand how the specific interactions affect the dispersion of graphite; therefore Raman spectroscopy experiments were performed to analyze the structural relationship of the graphite/UrCy-PPG composites, as presented in Fig. 1a. The signals in the Raman spectrum at around 2722 and 1578 cm^{-1} represent the 2D and G bands in graphite, respectively.[22,23] In the graphite/UrCy-PPG composite, the 2D band shifted gradually from 2722 cm^{-1} ($2D_2$) to 2692 cm^{-1} ($2D_1$) as the UrCy-PPG content increased. In addition, the G peak signal position was 1585 cm^{-1} (G') for all composites, which is 7 cm^{-1} higher than that of graphite. This difference is possibly due to the effect of the physical interactions between graphene and UrCy-PPG.[22] It should be noted that the small peak appearing at the D band intensity around 1347 cm^{-1} is considered to be a structural defect of disordered graphene, implying that natural graphite was successfully converted into graphene flakes by incorporating UrCy-PPG into the graphene layer.[22] Moreover, these structural defects of disordered graphene were calculated using the intensity ratio of the D and G bands (I_D/I_G). All I_D/I_G values were strongly dependent on the UrCy-PPG content, for instance in the 70/30 Graphite/UrCy-PPG composite, the I_D/I_G value was calculated to be 0.148. Upon further increasing the UrCy-PPG content to 7[illegible] wt%, the I_D/I_G value increased to 0.306, indicating the formation of single and few-layer graphene molecules.[24] This result further suggests that the number of graphene layers can be controlled by tuning the UrCy-PPG content of the composites; this feature has not been observed in previous studies.[14,25] Similar results were also obtained using X-ray photoelectron spectroscopy (XPS), as shown in Fig. S1. The C1s spectrum of graphite displayed a peak at 284.5 eV binding energy corresponding to C–C and C=C bonds,[26] while a higher binding energy and different positions for the C–C and C=C bonds were revealed in graphite/UrCy-PPG. Two new peaks belonging to UrCy-PPG composites, the C-N peak (287.4 ev) and the C=O peak (289.9 ev), appear to reflect the specific binding of graphene bound to the heteroatoms of UrCy-PPG. This implies the occurrence of effective intermolecular interactions between the p[illegible] groups of UrCy-PPG and the carbon sites of graphene. In addition, although point defects (vacancies) are created within the basal plane during the ultrasonic treatment,[27] the majorities of intermolecular interaction and pair correlation functions between graphene and UrCy-PPG are existed.

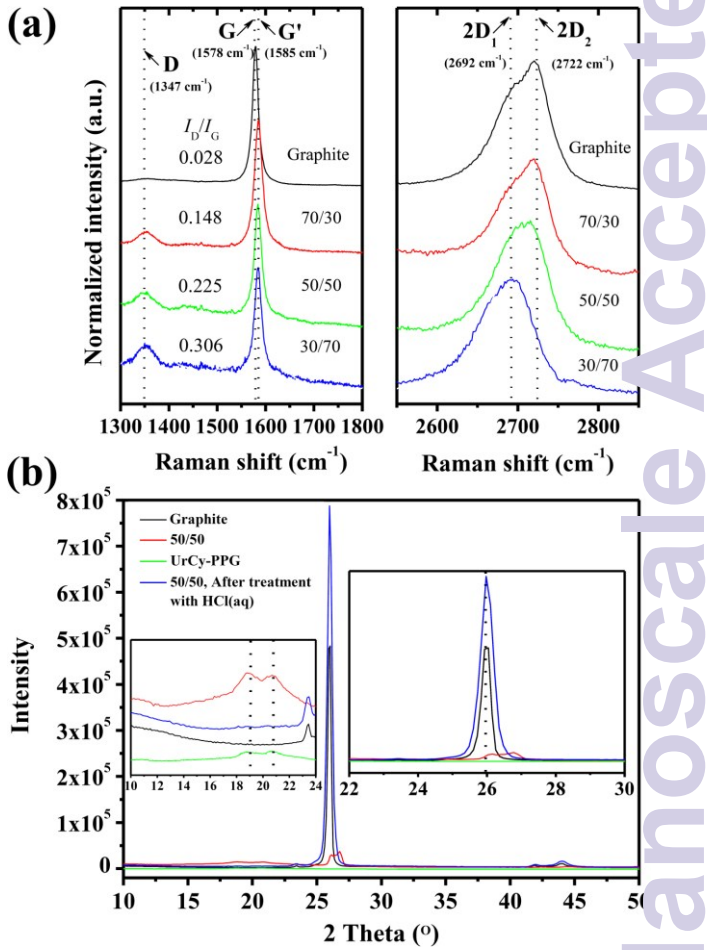

Fig. 1: (a) Raman spectra and **(b)** WAXD data for graphite, UrCy-PPG and graphite/UrCy-PPG hybrid composite in the solid state.

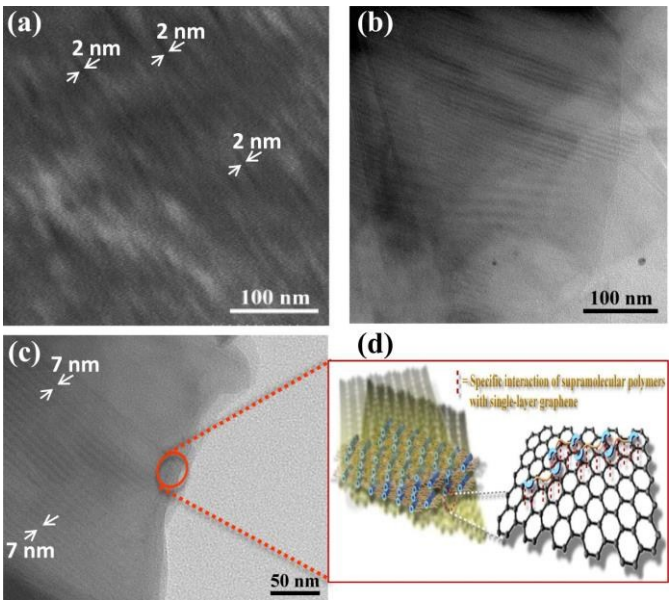

Fig. 2: (a) SEM cross-section image and **(b, c)** TEM images of 50/50 graphite/UrCy-PPG composite. **(d)** Schematic representation of supramolecular lamellar structures adsorbed on the graphene surface.

In order to confirm the existence of UrCy-PPG groups on the graphene surface, a series of wide-angle X-ray diffraction (WAXD) measurements were carried out. The WAXD patterns (Fig. 1b) revealed effective exfoliation of pristine graphite from graphite/UrCy-PPG composites; this was evident from disappearance of the graphite peak around 26° after the blending process. The weak peaks observed at 18.9° and 20.6° in the composite sample indicate the presence of orderly-packed UrCy segments and lamellar microstructures (see inset of Fig. 1b).[21] On the other hand, incorporating UrCy-PPG into the graphite matrix did not affect the supramolecular polymerization of UrCy-PPG due to the high association constant of the UrCy unit.[21] Thus, the influence of the supramolecular polymer on the formation of exfoliated graphite was investigated by examining the reactivity of the composite with aqueous hydrochloric acid (HCl); the acid may disrupt the self-complementary hydrogen bonding of UrCy-PPG, as shown in Fig. 1d. HCl completely returned the diffraction pattern of the graphite/UrCy-PPG composites to the original features of graphite, consistent with the Raman spectroscopy (Fig. S2). These results demonstrate the crucial importance of the presence of the UrCy end-functionalized hydrogen-bonded groups, which enable strong intermolecular interactions to form a stable supramolecular polymer and allow graphite to directly exfoliate into graphene. The non-covalent modification aids the UrCy self-interactions to improve the stability of the graphene suspension during the exfoliation process. Further investigation of the microstructures and morphologies of these composites was performed using electron microscopy techniques. The exfoliated structures of graphite/UrCy-PPG composites in the bulk state were observed using scanning electron microscopy (SEM) and transmission electron microscopy (TEM). In the 50/50 graphite/UrCy-PPG composite, the SEM image of the cross-section of the cleaved sample demonstrated a well-exfoliated morphology of graphene in the composite, with a thickness of approximately 2 nm, as shown in Fig. 2a. In addition, the length of the graphene flakes was longer than 500 nm, while the thickness remained constant. The TEM images in Figs. 2b and 2c indicate that the microstructures were well-arranged into lamellar-like patterns on the graphene surface, reflecting the growth of self-organized hierarchical UrCy-PPG complexes. The long period of the lamellar structure is ca. 7 nm wide, consistent with our previous observation.[21] The exfoliation mechanism of graphene is therefore suggested to occur via hierarchical self-assembly of UrCy-PPG, as illustrated in Fig. 2d and Scheme 3. The lamellar-like structures of UrCy-PPG are formed by stable π–π stacking of UrCy dimers that appear as a hard domain dispersed in a composite matrix. Formation of the hard domain can be used as an "adsorbent energy" source to exfoliate graphite and stabilize the produced graphene flakes in organic solvents. We suggest that this behavior can be attributed to the strong π-π interaction between graphene and UrCy-hard domain. In order to identify the number of graphene layers, atomic force microscopy (AFM) analysis was performed to measure the surface height profiles (Fig. 3). The images of the 50/50 graphite/UrCy-PPG composite suggested that the strip-like graphene flakes have lateral dimensions of 1–2 μm and exhibit well-dispersed patterns within individual graphene domains. The corresponding height profiles displayed in Figs. 3c and 3d present a non-uniform height over the range of 0.9-1.1 nm, showing the presence of adsorbed UrCy-PPG on the graphene surface. Since the theoretical thickness of single-layer graphene is only 0.34 nm, the thickness distribution of the produced graphene is suggested to be predominantly two or three layers, with adsorbed UrCy-PPG on the upper surface.

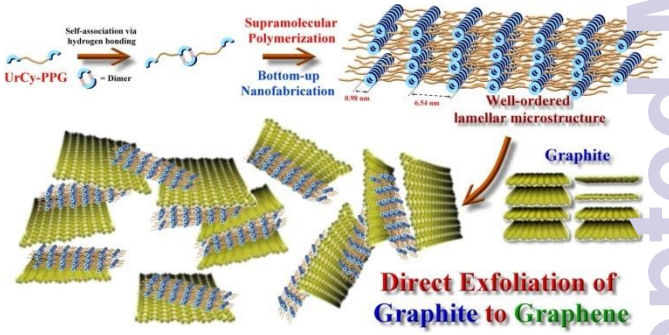

Scheme 3. Proposed mechanism for non-covalent exfoliation of graphene from graphite with UrCy-PPG.

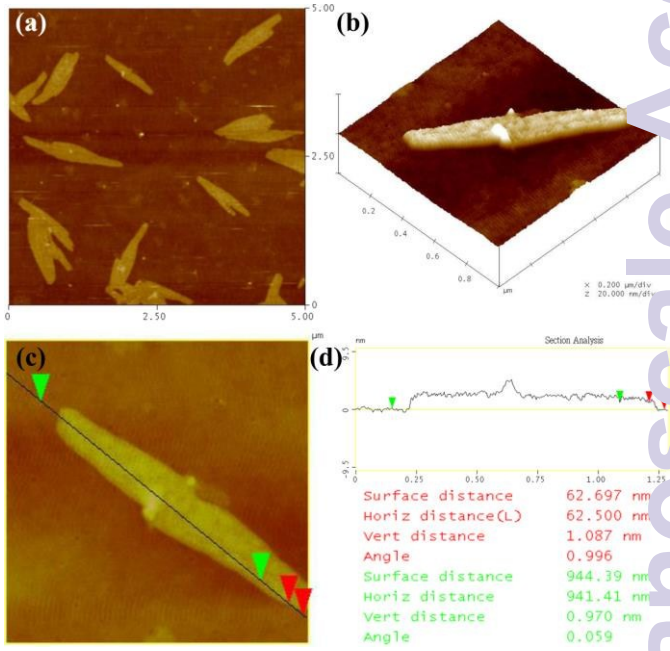

Fig. 3: (a) AFM images of 50/50 graphite/UrCy-PPG composite. **(c)** 3D representation of the surface shown in **(b)**. **(d)** Height profile of the AFM image corresponding to the line shown in **(c)**.

Temperature-dependent conductivity measurements provide an unprecedented insight into graphene-based electronic switches as this process is related to the operating conditions of the device. The conductivity of the graphite/UrCy-PPG composites was measured via AC impedance spectroscopy in a closed cell under low relative humidity (less than 30%). At 30 ℃, pristine UrCy-PPG has a very low conductivity (less than 10^{-10} S/m; Table S1) due to its natural insulating properties. When various amounts of UrCy-PPG were mixed with the graphite, conductivity gradually decreased as the UrCy-PPG content increased. The 50/50 graphite/UrCy-PPG composite exhibited a high conductivity of 1093 S/m, which was substantially higher than graphite (37 S/m) under the same conditions (Fig. 4a). The high conductivity of the graphene described in this work can be attributed to the interconnected conductive network constructed within the composite matrix.[28] Interestingly, all of the graphite/UrCy-PPG composites with different *wt%* ratios exhibited an obvious electrical transition and could be switched from a high conductivity state (the "ON" state) to a low conductivity state (the "OFF" state) during repeated cycles of heating and cooling between 30 ℃ and 100 ℃, due to the fact that the existence of the phase transition temperature (T = ~100 ℃) is contributed by non-covalent assembly of UrCy-PPG domains.[21] Fig. 4a illustrates that the ON/OFF ratio of the 30/70 composite exceeded 10^2, which was significantly higher than that of the 50/50 and 70/30 composites, indicating that volumetric thermal expansion of the composite increases gradually as the UrCy-PPG content increases. After multiple heating and cooling cycles, these composites displayed an exceptional temperature-dependent response and their conductive features nearly reverted back to the original values when the temperature decreased. Accordingly, Fig. 4b illustrates the thermoreversible transition from a well-connected graphene network to a more disordered liquid state, which results in a significant change in electrical conductivity. In addition, the melting enthalpy (ΔH) change for the different *wt%* ratios of the graphite/UrCy-PPG composites showed a similar trend as the ON/OFF switch (Figs. 4a and S3): the ΔH of the 30/70 composite (ΔH = 1.99 J/g) was higher than that of the 50/50 and 70/30 composites (ΔH = 1.21 and 0.96 J/g, respectively). Based on these results, the physical properties of graphite/UrCy-PPG composites, in particular their thermoreversible transition and temperature-dependent conductivity (compared to pristine graphite), have potential applications for graphene-based resistive-switching devices.

Conclusions

In summary, we have developed a simple, cost-effective and efficient method for the preparation of exfoliated graphene by direct exfoliation of graphite combined with the UrCy-PPG macromer in an organic solvent. Tuning the UrCy-PPG content of the composites can easily control the layer thickness of the exfoliated graphene flakes. Spectroscopic and microscopic studies demonstrated that the efficient interaction of UrCy-PPG with graphene results in the lamellar microstructure of adsorbed UrCy-PPGs on the graphite surface and strongly affects the exfoliation process and self-assembly behavior of graphene. In addition, the produced graphene composite exhibits a high conductivity (~1093 S/m) with a dramatic thermoresponsive ON/OFF resistance-switching behavior. Overall, this work indicates that the UrCy-PPG-based method can be usefully exploited to enable low-cost, mass production of exfoliated graphene, and may possibly provide a potential framework for developing graphene-based electronics for practical applications. The production of exfoliated graphene using a supramolecular polymer has not previously been proposed; therefore, this study represents state-of-the-art work. We are advancing further studies of the conduction mechanism[29] and computational simulation[30] of this system in the near future; these factors are generally believed to significantly affect electronic conductivity and device performance.

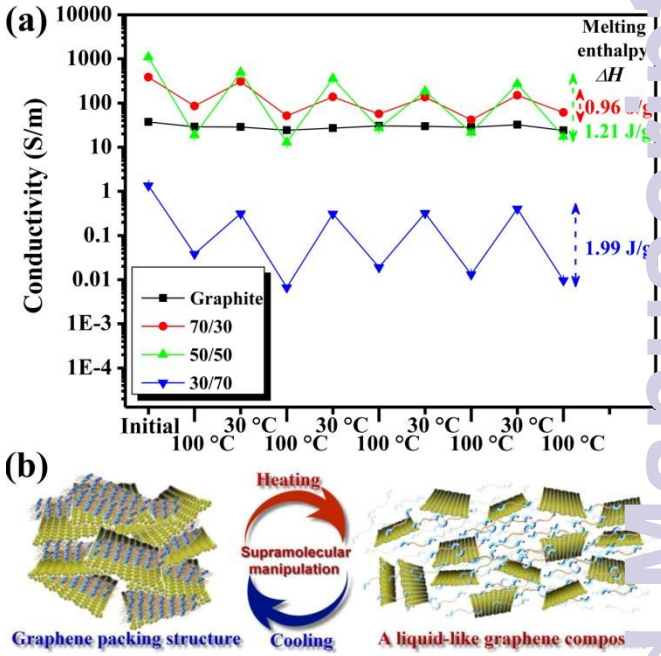

Fig. 4: (a) Temperature dependence of the electrical conductivity of the graphite/UrCy-PPG composites and graphite. **(b)** Suggested processes for the transition between the well-connected graphene network and disordered liquid state.

Acknowledgements

This study was supported financially by "Aim for the Top University Plan" of the National Taiwan University of Science and Technology and the Ministry of Science and Technology, Taiwan (contract no. MOST 104-2221-E-011-153).

Notes and references

1 J. C. Meyer, A. K. Geim, M. I. Katsnelson, K. S. Novoselov, T. J. Booth and S. Roth, *Nature*, 2007, **446**, 60.
2 C. Lee, X. D. Wei, J. W. Kysar and J. Hone, *Science*, 2008, **321**, 385.
3 A. A. Balandin, S. Ghosh, W. Z. Bao, I. Calizo, D. Teweldebrhan, F. Miao and C. N. Lau, *Nano Lett.*, 2008, **8**, 902.
4 C. N. R. Rao, A. K. Sood, K. S. Subrahmanyam and A. Govindaraj, *Angew. Chem. Int. Ed.*, 2009, **48**, 7752.
5 A. K. Geim and K. S. Novoselov. *Nat. Mater.*, 2007, **6**, 183.
6 (a) K.S. Kim, Y. Zhao, H. Jang and S. Y. Lee, *Nature*, 2009, **457**, 706.; (b) A. O'Neill, U. Khan, P. N. Nirmalraj, J. Boland and J. N Coleman, *J. Phys. Chem. C*, 2011, **115**, 5422.
7 (a) L. Chen, Y. Hernandez, X. Feng and K. Müllen, *Angew. Chem. Int. Ed.*, 2012, **51**, 7640.; (b) A. V. Alaferdov, A. Gholamipour-Shirazi, M. A. Canesqui, Yu. A. Danilov and S. A. Moshkalev, *Carbon*, 2014, **69**, 525.
8 T. Kuila, A. K. Mishra, P. Khanra, N.H. Kim and J. H. Lee, *Nanoscale*, 2013, **5**, 52.
9 A. N. Obraztsov, *Nat. Nano.*, 2009, **4**, 212.
10 Y. Zhang, L. Zhang and C. Zhou, *Acc. Chem. Res.*, 2013, **46**, 2329.
11 A, Ciesielski and P. Samorì, *Chem. Soc. Rev.*, 2014, **43**, 381.
12 Y. Xu, H. Bai, G. Lu, C. Li and G. Shi, *J. Am. Chem. Soc.*, 2008, **130**, 5856.
13 H Bai, Y Xu, L Zhao, C Li and G Shi. *Chem. Commun.*, 200

1667.
14 V. Georgakilas, M. Otyepka, A.B. Bourlinos, V. Chandra, N. Kim, K.C. Kemp, P. Hobza, R. Zboril and K.S. Kim, *Chem. Rev.*, 2012, **112**, 6156.
15 M. Matsumoto, Y. Saito, C. Park, T. Fukushima and T. Aida, *Nat. Chem.*, 2015, **7**, 730.
16 (a) F. Wang, C. Han, C. He, Q. Zhou, J. Zhang, C. Wang, N. Li and F. Huang, *J. Am. Chem. Soc.*, 2008, **130**, 11254.; (b) T. Aida, E. W. Meijer and S. I. Stupp, *Science*, 2012, **335**, 813. (c) X. Ji, S. Dong, P. Wei, D. Xia and F. Huang, *Adv. Mater.*, 2013, **25**, 5725.
17 F. Huang and O. A. Scherman. *Chem. Soc. Rev.*, 2012, **41**, 5879.
18 K. S. Chichak, A. Star, M. V. P. Altoé and J. F. Stoddart, *Small*, 2005, **1**, 452.
19 A. Ikeda, Y. Tanaka, K. Nobusawa and J.-I. Kikuchi, *Langmuir*, 2007, **23**, 10913.
20 A. Llanes-Pallas, K. Yoosaf, H. Traboulsi, J. Mohanraj, T. Seldrum, J. Dumont, A. Minoia, R. Lazzaroni, N. Armaroli and D. Bonifazi, *J. Am. Chem. Soc.*, 2011, **133**, 15412.
21 C. C. Cheng, F. C. Chang, J. H. Wang, Y. L. Chu, Y. S. Wang, D. J. Lee, W. T. Chuang and Z. Xin, *RSC Adv.*, 2015, **5**, 76451.
22 A. C. Ferrari,1, J. C. Meyer, V. Scardaci, C. Casiraghi, M. Lazzeri, F. Mauri,S. Piscanec, D. Jiang, K. S. Novoselov, S. Roth and A. K. Geim, *Phys. Rev. Lett.*, 2006, **97**, 187401.
23 K. H. Park, B. H. Kim, S. H. Song, J. Kwon, B. S. Kong, K. Kang and S. Jeon, *Nano Lett.*, 2012, **12**, 2871.
24 A.C. Ferrari, *Solid State Commun.*, 2007, **143**, 47.
25 Z. S. Wu, W. C. Ren, L. B. Gao, B. L. Liu, C. B. Jiang and H. M. Cheng, *Carbon*, 2009, 47, 493.
26 D. Yang, A. Velamakanni, G. Bozoklu, S. Park, M. Stoller, R. D. Piner, S. Stankovich, I. Jung, D. A. Field, C. A. Ventrice Jr. and R. S. Ruoff, *Carbon*, 2009, **47**, 145.
27 K. L. Lu, R. M. Lago, Y. K. Chen, M. L. H. Green, P. J. F. Harris and S. C. Tsang, *Carbon*, 1996, **34**, 814.
28 C. Wu, X. Huang, G. Wang, L. LV, G. Chen, G. Li and P. Jiang, *Adv. Funct. Mater.*, 2013, **23**, 506.
29 A. B. Kaiser, C. Gómez-Navarro, R. S. Sundaram, M. Burghard and K. Kern, *Nano Lett.*, 2009, **9**, 1787.
30 V. León, A. M. Rodriguez, P. Prieto, M. Prato and E. Vázquez, *ACS Nano*, 2014, **8**, 563.